Atmos. Chem. Phys. Discuss., 12, 12245–12285, 2012
www.atmos-chem-phys-discuss.net/12/12245/2012/
doi:10.5194/acpd-12-12245-2012

Atmospheric Chemistry and Physics Discussions

This discussion paper is/has been under review for the journal Atmospheric Chemistry and Physics (ACP). Please refer to the corresponding final paper in ACP if available.

The impact of differences in large-scale circulation output from climate models on the regional modeling of ozone and PM

A. M. M. Manders[1], E. van Meijgaard[2], A. C. Mues[3], R. Kranenburg[1], L. H. van Ulft[2], and M. Schaap[1]

[1]TNO, P.O. Box 80015, 3584 TA Utrecht, The Netherlands
[2]KNMI, De Bilt, The Netherlands
[3]FUB, Berlin, Germany

Received: 2 March 2012 – Accepted: 13 April 2012 – Published: 11 May 2012

Correspondence to: A. M. M. Manders (astrid.manders@tno.nl)

Published by Copernicus Publications on behalf of the European Geosciences Union.

Abstract

Climate change may have an impact on air quality (ozone, particulate matter) due to the strong dependency of air quality on meteorology. The effect is often studied using a global climate model (GCM) to produce meteorological fields that are subsequently used by chemical transport models. However, climate models themselves are subject to large uncertainties and fail to adequately reproduce the present-day climate. The present study illustrates the impact of this uncertainty on air quality. To this end, output from the SRES-A1B constraint transient runs with two GCMs, i.e. ECHAM5 and MIROC-hires, has been dynamically downscaled with the regional climate model RACMO2 and used to force a constant emission run with the chemistry transport model LOTOS-EUROS in a one-way coupled run covering the period 1970–2060.

Results from the two climate simulations have been compared with a RACMO2-LOTOS-EUROS (RLE) simulation forced by the ERA-Interim reanalysis for the period 1989–2009. Both RLE_ECHAM and RLE_MIROC showed considerable deviations from RLE_ERA in daily maximum temperature, precipitation and wind speed. Moreover, sign and magnitude of these deviations depended on the region. Differences in average concentrations for the present-day simulations were found of equal to (RLE_MIROC) or even larger than (RLE_ECHAM) the differences in concentration between present-day and future climate (2041–2060). The climate simulations agreed on a future increase in average summer ozone daily maximum concentrations (5–10 $\mu g\,m^{-3}$) in parts of Southern Europe and a smaller increase in Western and Central Europe. Annual average PM_{10} concentrations increased (0.5–1.0 $\mu g\,m^{-3}$) in North-West Europe and the Po Valley, but these numbers are rather uncertain. Overall, changes for PM_{10} were small, both positive and negative changes were found, and for many locations the two runs did not agree on the sign of the change. The approach taken here illustrates that results from individual climate runs can at best indicate tendencies and should therefore be interpreted with great care.

ACPD
12, 12245–12285, 2012

The impact of differences in large-scale circulation output

A. M. M. Manders et al.

1 Introduction

Ozone and particulate matter (PM) have an adverse impact on the health of human beings and other organisms. They also play a role in the climate system by their interaction with radiation and/or clouds (Raes et al., 2010; Zhang et al., 2010). The day-to-day and even sub-daily variability of concentrations strongly depends on atmospheric conditions, since these govern transport, dilution and deposition, as well as chemical conversions (cloud processes, photochemistry). For ozone, there is a strong correlation between ozone concentrations and temperature, the correlation of particulate matter with meteorological parameters is more complex and depends on the component (e.g. Tai et al., 2010; Jimenez-Guerrero et al., 2011; Manders et al., 2011; Mues et al., 2012). Due to changes in meteorology associated to a changing climate, ambient concentrations are expected to change even if anthropogenic emissions are kept constant. The quantification of expected changes in concentrations is highly relevant for policy making, as there are strict regulations for concentrations (e.g. EU (2008), US EPA NAAQS) and further emission reductions may be needed to comply with regulations under expected warmer conditions.

A common approach to study the impact of climate change on air quality is to directly use output of climate models in an air quality model (one-way coupling), with many examples for different meteorological models coupled to different air quality models, both at the global and the regional scale (e.g. Dentener et al., 2006; Forkel and Knoche, 2007; Giorgi and Meleux, 2007; Andersson et al., 2009). The overview by Jacob and Winner (2009) shows that the impact of climate change on air quality depends on the time horizon, region and component, and simulations with various models have resulted in either increases or decreases in concentration. Results generally show an increase in ozone concentration, related to an increase in temperature, whereas for PM results show weaker responses to changes in meteorology and are found less conclusive, with the different model simulations not even resulting in the same the sign of the change.

ACPD
12, 12245–12285, 2012

Climate models themselves are subject to considerable uncertainties due to assumptions and parameterizations and simplifications of processes. All climate models, both global and regional, have significant biases, which are different for each model and region (Christensen et al., 2007). They may represent for example too strong or too weak zonal flow. This is why a multi-model approach is crucial, and this approach is taken by IPCC. Despite the regional differences, there is a general consensus that there is global warming, with very likely an increase in frequency of hot extremes, heat waves and heavy precipitation and a poleward shift of extratropical storm tracks with consequent changes in wind, precipitation and temperature patterns (IPCC, 2007).

So far, the impact of biases in climate models on the outcomes of air quality modeling has not received much attention. A commonly applied assumption is that a climate model exhibits the same bias structure in both the present-day and the future climate simulation, so that concentration differences can be identified and interpreted straightforwardly. Most one-way coupled simulations only used one realization of the future climate, or two scenarios using the same climate model. But using two scenarios with the same climate model results in a change in amplitude of the change rather than shifts in patterns (Mitchell et al., 1999). Alternatively, Liao et al. (2007) produced a high and a low extreme of a meteorological baseline scenario, based on uncertainty estimates for the individual variables for future climate in terms of their probabilistic distributions. When results from an individual climate model are used, e.g. for flood predictions, bias-corrected precipitation fields are made prior to the application. However, it is very difficult to make *consistent* bias corrections for all meteorological fields at once, which would be required for use in air quality models.

To bypass the use of climate models, an extremely warm year in the present-day climate can be investigated as being representative for an average future year (Vautard et al., 2007a; Mues et al., 2012). This has the advantage that one can verify the ability of models to represent such conditions with observation (Mues et al., 2012), but in this way it is difficult to look into the variability of the future climate and obtain statistics about extremes. Another way is to directly manipulate the output of a meteorological model to

ACPD
12, 12245–12285, 2012

represent expected warmer future conditions (e.g. Im et al., 2011, 2012) and use that as input for the air quality model. The drawback of the latter method is that temperature, precipitation and wind are often modified independently and not in a dynamically consistent way. Therefore, these sensitivity studies can at most be used to identify the most relevant meteorological parameters for air quality, and indicate the possible change due to the change in this meteorological parameter. Since these changes do not simply add up for changes in e.g. temperature, wind and precipitation, it is only possible to arrive at qualitative results.

Owing to regional biases in global climate models and nonlinear responses of air quality to simulated climate change, results may strongly depend on which climate model is used. The present study aims to provide more insight in the differences in modeled ozone and PM concentrations when using different climate models. This is done by coupling the regional chemistry transport model LOTOS-EUROS to the regional climate model RACMO2. For the purpose of this study, two transient climate runs with RACMO2 have been carried out for the period 1970–2060. They were driven by boundary conditions from two different GCMs, i.e. ECHAM5 and MIROC-hires. Results were complemented by a present-day climate simulation for the period 1989–2009 forced by reanalysis data from ERA-Interim. While ECHAM5 and MIROC were both identified to be among the five best performing climate models in representing present-day climate conditions in Central Europe, their behaviour in terms of zonal mean flow is found rather different for present-day conditions as well as in climate change response, which has a strong impact on temperature and precipitation and the changes therein (Van Ulden and van Oldenborgh, 2006).

This study is limited to examining the impact of meteorology only, without feedback mechanisms. Therefore, constant anthropogenic emissions were used in LOTOS-EUROS. The impact of meteorology on biogenic and sea salt emissions is however included. The presented results are confined to analysis of long-term average ozone and PM_{10} concentrations over the European modeling domain and the present and future relationships between concentration and temperature. Model output from RACMO2

ACPD
12, 12245–12285, 2012

and LOTOS-EUROS is compared for two 20-yr periods, centered around 2000 and 2050, representing time slices of present-day and future climate conditions.

2 Description of models and method

2.1 RACMO2

RACMO2 is the regional atmospheric climate model of KNMI (Lenderink et al., 2003; Van Meijgaard et al., 2008). The RACMO 2.2 version used for this study consists of the 31r1 cycle of the ECMWF physics package embedded in the semi-Lagrangian dynamical kernel of the numerical weather prediction model HIRLAM and a few routines to link the dynamics and physics parts. It has participated in ensemble studies with other regional climate models (Jacob et al., 2007; Christensen and Christensen, 2007), which showed that the regional models did reproduce the large-scale circulation of the global driving model, albeit with biases, and that RACMO2 was not one of the extreme models.

RACMO2 employs a rotated longitude-latitude grid to ensure that the distance between neighboring grid points is more or less the same across the entire domain. For the coupled run a RACMO2 domain was configured just encompassing the standard LOTOS-EUROS domain (see Fig. 1). It has a horizontal resolution of 0.44° with 114 points distributed from 25.04° W to 24.68° E longitude and 100 points from 11.78° S to 31.78° N latitude in the rotated grid. The South Pole is rotated −47° in latitudinal direction and 15° in the longitude. In the vertical, 40 pressure levels were used. At this resolution RACMO2 uses a model time step of 15 min and output for coupling with LOTOS-EUROS was generated every three hours. The analysis of atmospheric parameters is limited to the interior of the RACMO2 domain, here obtained by omitting an 8-point wide boundary zone.

ACPD
12, 12245–12285, 2012

2.2 LOTOS-EUROS

LOTOS-EUROS is a Eulerian chemistry transport model on the European domain. It has participated in model intercomparison studies (Vautard et al., 2007b; Van Loon et al., 2007) and is well evaluated for PM_{10} in the Netherlands (Manders et al., 2009). It is used for the daily air quality forecast in the Netherlands and part of the MACC ensemble. Modeled species are ozone, nitrogen oxides, sulfur dioxide, ammonia, primary $PM_{2.5}$ and black carbon, primary PM_{10} (excluding $PM_{2.5}$ and black carbon), sulfate, nitrate, ammonium and sea salt and species relevant as precursors or reservoir (peroxy-acetylnitrate, volatile organic carbon). Total PM is defined as PM_{10} = PPM_{25} + PPM_{10}_coarse + BC + NO_3^-+$NH4^+$+SO_4^{2-} + 3.26*(Na_fine+Na_coarse).

The horizontal model domain was 10° W–40° E, 35–70° N on a 0.5 × 0.25° regular longitude-latitude grid. In the vertical 5 dynamical vertical layers up to 5 km were used, including a surface layer, a mixing layer and reservoir layers. For (photo)chemical gas reactions the CBM IV scheme is used, for secondary inorganic aerosol formation EQSAM is used. Friction velocity and Monin-Obukhov length could be taken from RACMO2 but are recalculated internally in LOTOS-EUROS for consistency with the grid size and land use in LOTOS-EUROS.

The regional model is driven from climatological boundary conditions for gases and aerosols. In the present set-up, these boundary conditions were kept constant for consistency, although background concentrations are expected to change. In the present study, anthropogenic emissions for 2005 (MACC 2005 emissions, Kuenen et al., 2011) were used for the whole period to isolate the effect of climate change. Natural emissions of sea salt and isoprene emissions by trees are calculated on line, they depend on wind speed (sea salt, Monahan et al., 1986) and temperature (isoprene, Guenther et al., 1993). Dust emissions, forest fire emissions and secondary organic aerosols were not included since they are either too uncertain (secondary organic aerosols), mainly fall outside the domain (dust) or cannot be modeled in a realistic way in a climate run (fire emissions).

ACPD
12, 12245–12285, 2012

For the climate simulations, 3-hourly instantaneous concentrations were stored to reduce the output. Since this may result in missing the daily maximum ozone concentration, this concentration was stored additionally.

2.3 Model runs and analysis method

RACMO2 and LOTOS-EUROS were configured to run along with each other. Three model runs were performed with RACMO2 downscaling the following meteorologies:

1. ERA-Interim boundaries, 1 January 1989–31 December 2009
2. ECHAM5r3 A1B scenario boundaries, transient, 1 January 1970–31 December 2060,
3. MIROC-hires A1B scenario boundaries, transient, 1 January 1970–31 December 2060.

In the text, these runs will be referred to as RLE_ERA, RLE_ECHAM and RLE_MIROC. Results from the period 1 January 1989 to 31 December 2009 (present-day climate) will be compared to identify biases, and the results for the period 1 January 2041 to 31 December 2060 (future climate) will be compared to the present-day results to study the impact of climate change. Due to the natural variability of the meteorology, it is important to compare long periods. A 20-yr period is chosen to compare with ERA-Interim, although in climate science the use of 30-yr periods is more common.

Climate model output is usually assessed using average temperatures and wind fields. However, these are not the most relevant parameters in studying the impact of climate on air quality. The following meteorological parameters are considered of particular relevance in relation to air quality:

– Daily maximum temperature. High temperatures go along with high ozone concentrations, both high and low temperatures are often related to stagnant conditions. In particular the number of summer days ($T_{max} > 25\,^{\circ}$C) is used. For some

ACPD
12, 12245–12285, 2012

regions low daily maximum temperatures ($T_{max} < 5\,^{\circ}C$) are related to stagnant conditions in winter.

- Wind speed. Low wind speed is related to stagnant conditions, in particular the number of calm days (daily average wind speed <2 $m\,s^{-1}$)
- Rain. Rain is related to wash-out of species, in particular the number of wet days. Since wet deposition is a very efficient removal process, the mere occurrence of precipitation is more important than its intensity and duration. To account for unphysical small amounts of drizzle that often occur in climate models, a threshold of 0.5 mm for daily accumulated rain was set.

These meteorological variables are not independent. For example very high and very low daily maximum temperatures are related to low wind speeds and little precipitation on most locations. Also, working with threshold values can exaggerate differences when there are many days with values around this threshold. Mixing height is an important variable for PM, and is determined by both temperature (convection) and wind (turbulence). In our analysis, it is represented indirectly by the temperature and wind speed.

To analyze long periods, long-term average values and their standard deviations were calculated for temperature, wind speed, rain and total PM concentrations. For ozone concentrations, the average daily maximum in summer (June, July, August) was calculated. Both spatial structures and time series at specific locations were investigated. These locations are a selection of major European cities and background locations (EMEP stations), see Fig. 1. Results will be illustrated for the locations Vredepeel and Madrid, which have the most contrasting signature. Vredepeel is in the south-east of the Netherlands in a rural area, but may be affected by the densely populated Randstad and nearby Ruhr area, and by local farming (in particular ammonia emissions). Its climate is moderate and affected by the sea. In contrast, Madrid is a large city in a much warmer and dryer climate, with high local NO_x and primary PM emissions. Tables with statistics, including the other stations, can be found in the Supplement. In addition

ACPD
12, 12245–12285, 2012

to the time averaged values, average relationships between temperature and rain, temperature and wind, and temperature and ozone and PM_{10} concentrations have been studied for the time series at these stations to see whether these relationships are different for the forcing GCMs and whether they change in response to climate change. To do this, all daily values per station were sorted on daily maximum temperature and subsequently averaged in 50 temperature bins. Since the temperature series are different for each model run and station, the temperature bins are different, but contain the same amount of data.

3 Results: meteorology

3.1 Behaviour of RACMO with ERA-Interim

As a first step, the meteorology of RACMO2 with ERA-Interim boundary conditions has been compared with ECMWF analysis meteorology for the period 2003–2007 (Manders et al., 2011). The correlation between the two meteorologies was fairly good, with correlations generally well above 0.9 for daily maximum temperature, and around 0.8 for daily average wind speed, with lower exceptions in mountainous areas. Only for daily cumulative rain the correlations were lower, around 0.5. Rain is notoriously difficult to model, and due to its discrete character small mismatches in space and time immediately lead to poor correlations. Annual mean precipitation was comparable, but the days on which it rained and the amounts of rain did not correspond well. RACMO2 tended to model slightly higher temperatures for the warmest episodes, resulting in more summer days ($T_{max} > 25\,^{\circ}$C) , but also simulated more winter days ($T_{max} < 5\,^{\circ}$C), so the temperature was slightly more variable. In particular in the Southern part of the domain, RLE_ERA tended to be too warm. The good correspondence for the largest part of the domain justifies the usage of RACMO with ERA-Interim as a baseline run for comparison with the two climate runs, although one should be aware that neither the

Discussion Paper | Discussion Paper | Discussion Paper | Discussion Paper |

ACPD

12, 12245–12285, 2012

The impact of differences in large-scale circulation output

A. M. M. Manders et al.

ECWMF analysis nor the ERA-Interim should be used as a substitute for observations, in particular for wind and precipitation.

3.2 Evaluation of climate runs

For the climate simulations, good day-to-day correlations between meteorology from RLE_ERA on the one hand and RLE_ECHAM or RLE_MIROC on the other hand cannot be expected, but for the present-day climate at least the frequency of occurrence of events and their amplitude should correspond. As a first indication, the average annual cycle for temperature, rain and wind speed was studied for a number of stations. In the Supplement, the statistics for a selection of locations is summarized.

3.2.1 General circulation

A first indication of the performance in representing the circulation can be derived from the average patterns of mean sea level pressure (mslp). As shown in Fig. 2a, the centers of low pressure during winter in both RLE_ECHAM and RLE_MIROC have shifted to the south compared to RLE_ERA, resulting in a more southerly average position of the Atlantic storm track. In RLE_ECHAM5, this shift extends to the whole of Western Europe giving rise to a stronger zonal circulation in this region compared to RLE_ERA. In RLE_MIROC, on the other hand, the center of low pressure is positioned much more to the west over the Central Atlantic which weakens its influence over the European landmass, resulting in a more frequent occurrence of stagnant conditions over the continent. Figure 2b shows that all simulations feature a prominent Azores anticyclone during summer, as expected. In RLE_ECHAM5, the simultaneous simulation of lower pressure on average over Northern Europe results in more frequent (north) westerly flow over Western Europe and very stable conditions over the Mediterranean. RLE_MIROC, on the other hand, is seen to overestimate mslp over Scandinavia and the North-East Atlantic which weakens the north-south pressure gradient and reduces the oceanic influence of the weather over the continent. This results in more stable summertime

ACPD
12, 12245–12285, 2012

conditions in Northern Europe and relatively more unsettled conditions in Southern Europe. Thus, in general, the circulation structures of RLE_ECHAM and RLE_MIROC have mutually different characteristics, but also with respect to RLE_ERA. On the other hand, it is also seen that differences between future climate and present-day climate within each of the transient runs are much smaller than the intermodel differences. The impact of these general findings on near-surface temperature and wind speed, and on precipitation will be discussed hereafter.

3.2.2 Temperature

For North-West Europe, the average daily maximum temperatures in summer derived from RLE_ECHAM for the present-day climate were up to 3 °C lower (e.g. Vredepeel) compared to RLE_ERA, also the number of days with $T_{max} > 25\,^{\circ}$C is much lower (Figs. 3 and S1, Table S1a). Annual average daily maximum temperatures between RLE_ECHAM and RLE_ERA differ less than the interannual variability from RLE_ERA, but restricted to the summer they differ more, with the exception the Spanish locations. Considering the period 2000 to 2050, the increase in annual average daily maximum temperature is larger than its interannual variability, but for the summer the increase is in the same order as the interannual variability. The future climate RLE_ECHAM summer temperatures were close to the present-day RLE_ERA summer temperatures. Also the seasonal cycle is weaker: the difference between summer and winter temperatures is smaller than for RLE_ERA (Fig. 4). For Southern Europe, the temperatures resemble those of RLE_ERA more closely.

The difference in annual mean and summer mean daily maximum temperature between RLE_MIROC and RLE_ERA is smaller than the interannual variability, with the exception of the Spanish stations. The difference between future and present-day annual and summer average daily maximum temperature is larger than the interannual variability for all stations. Temperatures from RLE_MIROC corresponded better to the present-day summer and summer-winter difference than RLE_ECHAM, but tended to be somewhat higher than RLE_ERA (2 °C) in early summer for North-West Europe.

ACPD
12, 12245–12285, 2012

Also in the future climate RLE_MIROC gives a 2 °C higher average summer daily maximum temperature compared to RLE_ECHAM. However, for South Europe RLE_MIROC tends to be the coldest model. For example focusing on Spain, RLE_MIROC clearly had the lowest temperatures in present-day summer, whereas in the future climate the temperatures from RLE_MIROC and RLE_ECHAM become comparable in summer, autumn and early winter. In future late winter/early spring, RLE_MIROC is warmer than RLE_ECHAM. This is also reflected in Fig. 3, which shows that RLE_ERA yielded more warm days than RLE_ECHAM in a broad region around 50° N, the Sahara and the Mediterranean, whereas RLE_MIROC is comparable to the run using RLE_ERA in North-West Europe, much warmer in Russia and parts over the Mediterranean Sea, but on the other hand much colder in the Mediterranean countries. For the future climate, both simulations show an increase in summer days with a clear North-South gradient, but the changes are much larger for RLE_MIROC than for RLE_ECHAM.

3.2.3 Precipitation

RLE_ECHAM and RLE_MIROC both produce more precipitation than RLE_ERA, with RLE_ECHAM being the wettest nearly everywhere (Table S1b). RLE_ECHAM produces a larger number of wet days in Western Europe than RLE_ERA, but it has less wet days near Norway and the Eastern Mediterranean and around the Black Sea (Fig. 5, Table S1b). For RLE_MIROC however, the number of wet days in Northern Europe, north of 50° N is smaller than for RLE_ERA, while it is larger south of this latitude. The difference between future and present-day climate is comparable for the two transient runs, with less precipitation in the Mediterranean area and somewhat more rain in Central and Northern Europe, with a slightly stronger signal for RLE_MIROC in the Mediterranean. The annual cycle of monthly mean precipitation (Fig. 4) shows the same general pattern for the several model runs and time windows. For North-West Europe (e.g. Vredepeel), the amount of precipitation is relatively constant throughout the year. RLE_ECHAM is clearly wettest, with little difference between present-day for the first half of the year and larger differences in the second half. RLE_MIROC is close

ACPD
12, 12245–12285, 2012

to RLE_ERA for the present-day climate, except for late summer when it is wetter. For the future climate, RLE_MIROC becomes wetter, except for the late summer period. So in a future climate both transient runs generate a wetter spring/early summer and little change in autumn. For South-West Europe, (e.g. Madrid), there is a clear annual cycle, with dry summer months and a wet winter period. For Madrid, RLE_ECHAM 2041–2060 is the most extreme case, with over 100 mm more rain in January than in June. In contrast, RLE_MIROC 1989–2009 shows very little variation during the year. For a location in North-West Europe, both models yield drier spring, summer and autumn seasons and wetter winters.

3.2.4 Wind speed

According to the model, 10-m wind speed in mountainous regions is in general lower than in lower elevated, flat areas. This is clearly illustrated by the spatial distribution of the annual mean number of calm days for RLE_ERA in Fig. 6. Such model behavior is owing to the high value of surface roughness length for momentum associated with mountainous terrain. While the contrast in number of calm days between flat and mountainous areas might not be confirmed by observations we want to emphasize that this study deals with differences or changes, and not with absolute values. All 10-m wind speed output has been obtained with the same surface roughness map which considerably helps in the interpretation of the relative differences.

For the present-day climate, the number of calm days for RLE_ECHAM is comparable to that for RLE_ERA in Northern Europe, but RLE_ERA gives more calm days in Central and Southern Europe, and at the eastern boundary of the domain (Fig. 6). RLE_MIROC tends to give more calm days than RLE_ERA, except in North-West Africa and at the eastern boundary of the domain. The difference between future and present-day climate is small in both transient simulations, less than 10 days on average, slightly more for RLE_MIROC which has more calm days and in larger areas in the future climate, with local exceptions. Also the resulting annual cycles of wind speeds are comparable (Fig. 4). For North-West Europe (e.g. Vredepeel), RLE_ERA is in between

RLE_ECHAM (more wind) and RLE_MIROC (less wind), with the largest differences in summer which, as shown in Fig. 4, is the period with lowest wind speed. Also in the time series at Vredepeel there appears to be little difference between present-day and future climate. For South West Europe (e.g. Madrid), wind speeds tend to be lower, and are constant throughout the year for RLE_ERA. The transient simulations show a weak annual cycle, with more wind in (late) winter but comparable wind speeds in summer. RLE_ECHAM deviates most from RLE_ERA. Again, the difference between present-day and future average wind speed is very small in both transient simulations.

For all selected meteorological parameters, differences are not only a shift in amplitude, but also in pattern. Results are consistent with the conclusions for a model intercomparison for the global models' present-day climate (Van Ulden and Van Oldenborgh, 2006). ECHAM5 was found to have less easterly flow than the observed present-day climate, whereas MIROC tended to be more stagnant, which has a direct impact on temperature and rain. The output from two global models was found rather consistent concerning the simulated change in annual mean temperature across Europe, but differed considerably in seasonality.

4 Results: concentrations of ozone and PM_{10}

4.1 Present-day climates

For ozone, the summer average daily maximum (June-July-August) was studied (Figs. 7, S1). There is a general north-south gradient. Concentrations are largest above the Mediterranean Sea (up to 150 µg m^{-3}), followed by lower concentrations (110 µg m^{-3}) in industrial areas in southern Europe (Po Valley, around Porto, Rhone delta) and in Central Europe. For PM_{10}, concentrations are largest in densely populated and industrialized areas (The Netherlands, Ruhr area, Po Valley), Poland and major cities, and above the sea, due to the high local contribution of sea salt. Lowest concentrations were found above Scandinavia, Eastern Europe, Balkan, Ireland,

ACPD
12, 12245–12285, 2012

Scotland, parts of Spain and Northern Africa. The low concentrations are partly unrealistic, since no dust and secondary organic aerosol was taken into account. These components may contribute significantly to PM in southern Europe.

For the present-day climate, summer ozone concentrations in the RLE_ECHAM run are up to 12 $\mu g\,m^{-3}$ lower than in the RLE_ERA run in a large part of the domain (Fig. 8, Fig. S1), in particular in North-West Europe, the Baltic Sea region and the Mediterranean area. Only in a few small areas at the southern boundary of the domain, RLE_ECHAM yields higher concentrations. For RLE_MIROC it is the other way round, with up to 12 $\mu g\,m^{-3}$ higher concentrations in North-West Europe and higher concentrations in specific areas around the Mediterranean Sea. In the present-day part of both transient simulations, the pattern of the difference is not clearly related to the patterns of ozone concentrations, indicating a shift in patterns rather than only differences in amplitude. This is consistent with the notion that changes in meteorological conditions can (in part) be associated to changes in patterns. The differences in ozone concentration with the RLE_ERA result can only in part be related to the patterns of number of summer days, since the sensitivity of ozone to temperature depends on the location and the temperature, as will be illustrated further on. Relative differences (not shown) have a spatial pattern that follows the pattern of absolute differences. Over sea, they are up to 20 % in both models, in particular at the ship tracks, whereas over land relative differences are less than 10 %. For RLE_ECHAM, the difference with RLE_ERA is larger than the interannual variability, except for the Spanish stations, while for RLE_MIROC the difference with RLE_ERA tends to be smaller than the interannual variability (Fig. S1).

Over land, simulated total PM_{10} concentrations in the present-day part of both transient runs are lower than in the RLE_ERA run, with the difference for RLE_ECHAM being much larger than for RLE_MIROC, with the exception of specific locations in Russia (Fig. 9). The patterns of differences in PM_{10} concentrations between RLE_ECHAM and RLE_ERA can be related to the patterns of reduced number of calm days (Fig. 6). For RLE_MIROC, differences are smaller and the increase in number of wet days

ACPD
12, 12245–12285, 2012

may contribute more to the lower PM_{10} concentrations seen in this simulation. Over sea, the differences in total PM_{10} is particularly large, and can easily be related to wind-generated sea salt. Sea salt aerosol generation depends strongly on the 10 m wind speed (Monahan et al 1989). In the Northern seas, RLE_MIROC tends to have lower wind speeds (not shown) than RLE_ERA and RLE_ECHAM, leading to reduced sea salt emission. In the Mediterranean area, the wind speed tends to be lower in RLE_ERA than in RLE_ECHAM or RLE_MIROC (less calm days, Fig. 6, wind speeds for Barcelona, Table S1c), leading to more sea salt generation in the latter simulations. In RLE_ECHAM this effect is reinforced by a decrease in number of wet days, leading to less wet deposition, whereas in RLE_MIROC the increase in precipitation counter-balances the increase in sea salt aerosol production in part so that the concentration differences are smaller than for RLE_ECHAM. Relative differences (not shown) are up to 25 %, following the spatial patterns of the absolute differences, except for Scandinavia where very low PM concentrations are found, resulting in large relative differences. The differences between RLE_ERA and RLE_ECHAM are equal to or larger than the interannual variability, while for RLE_MIROC the differences are smaller than the interannual variability (Fig. S1).

4.2 Concentration changes due to climate change

Both RLE_ECHAM and RLE_MIROC show an increase in average O_3 summer maximum concentrations, up to 12 $\mu g\,m^{-3}$ (Fig. 8), but these differences are found over much larger areas in the RLE_MIROC simulation which is consistent with the finding in Fig. 3. This figure illustrates that the amount of increase in average maximum temperature depends both on the model and the region, with changes in RLE_MIROC larger and more widespread than in RLE_ECHAM leading to larger responses in ozone concentration. Moreover, the change in ozone concentration with temperature depends on the region since it is dependent on the availability of NO_x and VOC, so that the same temperature changes may lead to different changes in concentration for different regions. This point is further illustrated in the nex section. Relative differences

ACPD
12, 12245–12285, 2012

with the present-day climate simulation are up to 5 % for RLE_ECHAM and up to 10 % for RLE_MIROC. Again, patterns closely follow those of the absolute differences. For RLE_ECHAM, the difference in concentration between future and present-day is smaller than the interannual variability in North Europe and about equal to the interannual variability in South Europe. For RLE_MIROC the difference induced by climate change is larger than the interannual variability (Fig. S1).

Differences in PM_{10} concentrations between future and present-day climate are rather small. For RLE_ECHAM, concentrations are up to 2 $\mu g\,m^{-3}$ lower above the Atlantic east of Norway, which could be a combined effect of more precipitation in that region in the future climate (more wet deposition) and lower wind speeds (less sea salt generation). Differences over the continent are very small (less than 0.5 $\mu g\,m^{-3}$), except for a small area around Moscow,where concentrations have decreased by more than 2 $\mu g\,m^{-3}$. For the RLE_MIROC run, differences above the continent are somewhat larger but still small (increases in concentration of up to 0.7 $\mu g\,m^{-3}$ in the Netherlands and theNorth-East of Spain, with a maximum of 2 $\mu g\,m^{-3}$ in the Po Valley, and a distinctl decrease in concentrations around Moscow). Relative differences are less than 10 % for RLE_ECHAM and up to 10 % for RLE_MIROC, with patterns related to the patterns of absolute differences. Only for Scandinavia the small absolute differences still yield relatively large relative differences because of the low absolute concentrations. For both RLE_ECHAM and RLE_MIROC the changes in PM_{10} concentrations corresponding to climate change differences are smaller than the present-day interannual variability derived for the analysed locations (Fig. S1).

4.3 Changes in average correlations between temperature and ozone or PM_{10} concentrations

The average relationships between ozone or PM_{10} concentrations on the one hand and temperature on the other hand have been investigated for several sites. The results are again illustrated for Vredepeel and Madrid (Fig. 10). For each site the general

ACPD
12, 12245–12285, 2012

tendencies are similar for the different model simulations, but there are notable differences between the various sites.

For ozone the relationship with temperature is very distinct and has little scatter. There is a gradual increase with temperature, but the slope is not constant with temperature, while the size of the slope depends on the location. For Vredepeel for example, the slope seems to be somewhat steeper for temperatures above 20 °C whereas for Madrid, the figure shows a steep increase for moderate temperature and a levelling-off for temperatures above 20 °C. The value of the slope also differes slightly per model run. The highest concentrations in Madrid are nearly 40 $\mu g\,m^{-3}$ lower than in Vredepeel, in spite of the higher temperatures. This difference in maximum concentration for high daily maximum temperature does not contradict the mean North-South gradient in mean O_3 concentrations with higher concentrations in the South. The reason is thats the high temperatures favouring high ozone concentration occur more frequently in the South. The levelling-off is not seen to this extent at the other locations, like Barcelona or Paris. The difference in slope between the locations can be attributed in part to the local NO_x/VOC ratio. In the Netherlands, ozone production is VOC-limited, and the increased VOC emissions from trees at higher temperatures accelerates the increase in ozone concentrations, leading to a steeper increase of ozone concentration with temperature. In contrast, on the Iberian peninsula, the ozone formation is generally NO_x-limited, and a deep boundary layer associated to fair weather may result in more dilution. Moreover, for Madrid the local NO_x emissions contribute to the local destruction of ozone (titration).

Total PM_{10} concentrations at Vredepeel show a minumum value around a daily maximum temperature of 10 °C. For Madrid, PM_{10} concentrations have their maximum at around 17 °C with linear decreases for both higher and lower temperatures, with an exception for the coldest days when the concentrations have relatively high values. These differences may have several causes. The differences in simulated PM_{10} concentration can be related to differences in wind speed and precipitation versus temperature, with higher wind speeds (mixing) and precipitiation (wet deposition) for temperatures

ACPD
12, 12245–12285, 2012

around 12 °C for Vredepeel, explaining the PM minimum. In contrast, for Madrid higher wind speeds and precipitation are associated to nearly the lowest temperatures. The decrease in PM_{10} concentration for higher temperatures is counter-intuitive, since at these temperatures wind speeds and precipitation are generally lower than on average. On the other hand, at high temperatures the mixing layer is expected to be deeper, leading to more dilution. The effect may in part be due to the relatively coarse grid resolution, which may result in considerable dilution of the Madrid emissions since it is surrounded by areas with low concentrations. In that case, the results may strongly depend on the wind direction, which we did not take into account in our analysis since it is a local relationship. An indication for this is the large scatter in PM_{10} for Madrid. A second cause may be the contribution of the different components of PM_{10} (not shown). In Vredepeel, ammonium and nitrate concentrations are higher, due to nearby ammonia emmissions from farming. There, temperature-dependent reactions involving secondary inorganic aerosol and the volatility of ammonium nitrate may have an impact. In contrast, in Madrid the inert black carbon concentrations contribute most and concentrations are more directly determined by dilution, transport and deposition For other locations (not shown) the behaviour is seen somewhat in-between the illustrated results, with in general higher PM values for lower temperatures, a minimum for temperatures around 15 °C, but not everywhere the increase with temperature for high temperatures was reproduced. The large scatter indicates that the relationship between PM and meteorology is complex and that using only temperature as a proxy for meteorological conditions is not all-explanatory.

Maximum concentrations in ozone are reached in summer since ozone is formed by photochemical reactions. For PM_{10}, the annual cycle depends on the exact composition which varies per location. To investigate the annual cycle and periods in which the impact of climate change is largest, we analyzed the 20-yr records of monthly mean PM_{10} concentration simulated for Vredepeel and Madrid (Fig. 11). PM_{10} concentrations tend to be lowest in summer. Some locations show distinct periods of higher concentrations in spring/autumn (Melpitz, Barcelona), others show a more gradual

Discussion Paper | Discussion Paper | Discussion Paper | Discussion Paper |

ACPD

12, 12245–12285, 2012

The impact of differences in large-scale circulation output

A. M. M. Manders et al.

increase in the winter half year. For Madrid, modelled high PM_{10} concentrations are a winter phenomenon, with the highest concentrations seen in the RLE_ERA run (with the lowest wind speeds and least precipitation in the winter months). Vredepeel however has rather high PM_{10} concentrations in early spring and late summer. This can be partly related to the relatively high ammonia emission for this area in this time of the year, and partly to wind speed, in particular for the RLE_MIROC future climate, which has the lowest wind speeds in late summer. Also the RLE_ECHAM run shows an increase in PM_{10} concentrations due to climate change for late summer in Vredepeel. For Madrid, RLE_MIROC and RLE_ECHAM give concentration changes due to climate change of up to 2 $\mu g\,m^{-3}$ but with opposite sign, decreasing future PM_{10} concentrations for RLE_MIROC and increasing concentrations for RLE_ECHAM5. The differences in annual mean concentrations can be lower than the difference in monthly mean concentrations, since the latter can partly cancel out for a full year.

5 Discussion and conclusions

Two long-term climate simulations have been performed with the one-way coupled system RACMO2-LOTOS-EUROS, using meteorological boundary coditions from two different GCMs. The results are used to compute the difference in air quality between the present-day (1989–2009) and the future climate (2041–2060). The future-climate simulations yield an increase in mean daily summer maximum ozone concentrations, with increases of up to 12 $\mu g\,m^{-3}$. Future climate annual mean PM_{10} concentrations are found up to 1–2 $\mu g\,m^{-3}$ lower above the Northern Atlantic, whereas over the continent differences are in the order of 0.5 $\mu g\,m^{-3}$ with positive differences over the Netherlands and North-West Germany, North-East Spain and the Po valley. Results from the two simulations are in agreement regarding general response (general increase in ozone concentration, weak response of PM_{10}), but showed considerable differences in absolute values and between regions, in particular for PM_{10} for some regions the two

Discussion Paper | Discussion Paper | Discussion Paper | Discussion Paper |

ACPD

12, 12245–12285, 2012

The impact of differences in large-scale circulation output

A. M. M. Manders et al.

models did not even agree on the sign of the change. Changes for PM_{10} are smaller than the interannual variability.

It is not straightforward to compare the results derived in this paper with results from literature, due to the differences in metrics used (e.g. average 8-h maximum, averages over April–September, AOT40), the difference in time windows (most used are 1961–1990, 2071–2100), and differences in climate scenario (A2, A1B). Nevertheless, the results of this study appear to be generally in line with European studies (e.g. Giorgi and Meleux 2007, up to 10 ppbv difference in mean daily summer ozone concentrations, Andersson et al., 2009, up to 7 ppbv difference in mean daily maximum O_3, 2021–2050, Carvalho et al. (2010) are at the high end with up to 50 $\mu g\,m^{-3}$ difference in monthly mean O_3 concentrations) and US studies (see the overview by Jacob and Winner, 2009). For PM, annual or seasonal means are usually reported, but results are sometimes given per component, with changes up to 10 %, or less than 1 $\mu g\,m^{-3}$ (Jacob and Winner, 2009), with both increases and decreases.

The changes in concentrations of ozone and PM_{10} can be related to changes in temperature, in particular daily maximum temperature, and to a lesser extent to changes in precipitation and wind speed. Average relationships are found slightly different for the different simulations and time windows. This implies that average relationships for the present-day climate cannot be directly extrapolated to the future. Furthermore changes are not uniform over the year. High ozone concentrations are clearly a summer phenomenon but for PM_{10} seasonal behaviour is less uniform. For example, the finding of an increase in summertime PM_{10} for the Netherlands seems a robust feature, but fot other seasons the changes appear smaller, while for Madrid the model simulations indicate that high PM_{10} concentrations in that region are mainly a winter phenomenon.

Comparing the simulations for the period 1989–2009 showed that RLE_ECHAM and RLE_MIROC both have considerable biases with respect to RLE_ERA, depending on the season and region. This is in spite of the fact that both ECHAM5 and MIROC are among the well-performing global climate models. These biases have a substantial impact on the modelled ozone and PM_{10} concentrations: differences in

ACPD
12, 12245–12285, 2012

A. M. M. Manders et al.

modelled concentrations between future and present-day climate are found smaller than the differences in present-day climate between RLE_ECHAM5 and RLE_ERA. In the RLE_MIROC simulation, the differences between future and present-day climate are of comparable order of magnitude as the present-day differences between the simulations of RLE_MIROC and RLE_ERA. Biases for RLE_ECHAM and RLE_MIROC are different, illustrating the uncertainties in the global climate models. Results from a single transient simulation should therefore be interpreted in a qualitative rather than a quantitative way, as an illustration of one out of many possible climate change realisations. The two simulations analyzed in this paper show both differences and consistent changes related to climate change, but ideally an ensemble approach should be taken, with ensemble members from different GCMs and different regional climate models.

The chemistry transport model also has biases, and a good ensemble would include several CTMs. LOTOS-EUROS underestimates the daily ozone maximum (Curier et al., 2012), in particular the highest ozone peaks ($180\,\mu g\,m^{-3}$) are underestimated by 10–$20\,\mu g\,m^{-3}$. It also underestimates total PM_{10}, in particular in summer (Manders et al., 2009). In Mues et al. (2012) the relation between temperature and PM_{10} concentrations was investigated for LOTOS-EUROS and compared with observed concentrations. The observed increase of PM concentrations with temperature was not represented to the same extent by the model. For winter periods, for which PM is mainly determined by ventilation effects, the behaviour is fairly good, but in summer the model did not perform well. LOTOS-EUROS lacks a good description of SOA, which may contribute significantly (typically up to a few $\mu g\,m^{-3}$) in summer through the temperature dependency of biogenic emissions and the dependency on photochemistry (oxidation) and volatility (Donahue et al., 2009 and references therein). Also windblown dust will be more important under warmer and dryer conditions, in particular in southern Europe, and is not taken into account. Furthermore, the contribution of forest fire emissions is not modelled. Forest fires can contribute significantly to ozone and PM concentrations during fire episodes and can cause serious and acute local air quality problems. In addition, long-range transport of the fire emissions has an impact on atmospheric conditions at

ACPD
12, 12245–12285, 2012

distances of hundreds of kilometers away from the fire, not only on the concentrations but also on the radiation budget and atmospheric stability (e.g. Hodzic et al., 2007; Saarikoski et al., 2007). Also the emissions of forest fires are expected to increase for a warmer climate in the Mediterranean area (e.g. Moriondo et al., 2006).

In the present study, anthropogenic emissions have been kept constant at the 2005 level to facilitate focussing on the impact of meteorology. The interannual variability in concentration is largely due to meteorological variability rather than interannual variability in emissions (Andersson et al., 2007), but the effect of emission differences between 2000 and 2050 on long-term average concentrations may be as large as or even larger than the effect of climate change (Tagaris et al., 2007). Not only the amount of emissions, but also their timing may change, due to changes in energy sources and in human activity patterns. The increase of observed EC concentrations with higher temperatures that was not reproduced by LOTOS-EUROS (Mues et al., 2012) may indicate a relationship between of meteorology on anthropogenic emissions. Therefore, emission scenarios should be taken into account when assessing air quality for a future period.

Other sources of uncertainty for climate change-air quality interactions are the boundary conditions, enhanced stratosphere-troposphere exchange and higher background levels. Andersson et al. (2009) conducted an impact study, and Hogrefe et al. (2011) studied the uncertainties associated with chemical boundary conditions from a global model, showing that the interannual variability was underestimated when time-invariant boundary conditions were used. Also land use changes may be relevant, both changing deposition efficiencies and biogenic emissions, although their effect may be small. And last but not least, two-way interactions between concentrations of species and the radiation budget of the atmosphere should be taken into account (Zhang et al., 2010) but most coupled models cannot perform long-term climate studies due to the large computational effort that would be required. A two-way coupling is currently being realised in the RACMO2-LOTOS-EUROS system.

ACPD
12, 12245–12285, 2012

Supplementary material related to this article is available online at: http://www.atmos-chem-phys-discuss.net/12/12245/2012/ acpd-12-12245-2012-supplement.pdf.

Acknowledgements. This project was supported by the Dutch Knowledge for Climate Programme.

References

Andersson, C., Langner, J., and Bergstrom, R.: Interannual variations and trends in air pollution over Europe due to cllimate variability during 1958–2001 simulated with a regional CTM coupled to the ERA-40 reanalysis, Tellus, 59B, 77–98, 2007.

Andersson, C.: Air pollution dependency on climate variability and source region, PhD. Thesis, Stockholm University, 2009.

Carvalho, A., Monteiro, A., Solman, S., Miranda, A. I., and Borrego, C.: Climate-driven changes in air quality over Europe by the end of the 21st century, with special reference to Portugal, Environ. Sci. Policy, I3, 445–458, 2010.

Christensen, J. H. and Christensen, O. B.: A summary of the PRUDENCE model projections of changes in European climate by the end of this century, Climate Change, 81, 7–30, 2007.

Curier, R. L., Timmermans, R., Eskes, H., Calabretta-Jongen, S., Segers, A., and Schaap, M.: Improving ozone forecasts over Europe by synergistic use of the LOTOS-EUROS chemical transport model and in-situ measurements, Atmos. Environ., submitted, 2012.

Dentener, F., Stevenson, D., Ellingsen, K., Van Noije, T., Schultz, M., Amann, M., Atherton, C. L., Bell, N., Bergmann, D. L., Bey, I., Bouwman, L., Butler, T., Cofala, J. D., Collins, B., Drevet, J., Doherty, R., Eickhout, B., Eskes, H., Fiore, A., Gauss, M., Hauglustaine, D., Horowitz, L., Isaksen, I. S. A., Josse, B., Lawrence, M., Krol, M., Lamarque, J. F., Montanaro, V., Müller, J. F., Peuch, V. H., Pitari, G., Pyle, J., Rast, S., Rodriguez, J., Sanderson, M., Savage, N. H., Shindell, D., Strahan, S., Szopa, S., Sudo, K., Van Dingenen, R., Wild, O., and Zeng, G.: The global atmospheric environment for the next generation, Environ. Sci. Technol., 40, 3586–3594, 2006.

ACPD

12, 12245–12285, 2012

Donahue, N. M., Robinson, A. L., and Pandis, S. N.: Atmospheric organic particulate matter : From smoke to secondary aerosol, Atmos. Environ., 43, 94–106, 2009.
EPA: National Ambient Air Quality Standards, available at: http://www.epa.gov/ttn/naaqs/ EU Directive 2008/50/EC of the European Parliament and of the Council of 21 May 2008 on ambient air quality and cleaner air for Europe, 2008.
Giorgi, F. and Meleux, F.: Modelling the regional effects of climate change on air quality, C.R. Geoscience, 721–733, 2007.
Guenther, A. B., Zimmerman, P. R., Harley, P. C., Monson, R. K., and Fall, R.: Isoprene and monoterpene emission rate variability: model evaluations and sensitivity analyses, J. Geophys. Res., 98, 12609–12617, 1993.
Hodzic, A., Madronich, S., Bohn, B., Massie, S., Menut, L., and Wiedinmyer, C.: Wildfire particulate matter in Europe during summer 2003: meso-scale modeling of smoke emissions, transport and radiative effects, Atmos. Chem. Phys., 7, 4043–4064, doi:10.5194/acp-7-4043-2007, 2007.
Hogrefe, C., Hao, W., Zalewsky, E. E., Ku, J.-Y., Lynn, B., Rosenzweig, C., Schultz, M. G., Rast, S., Newchurch, M. J., Wang, L., Kinney, P. L., and Sistla, G.: An analysis of long-term regional-scale ozone simulations over the Northeastern United States: variability and trends, Atmos. Chem. Phys., 11, 567–582, doi:10.5194/acp-11-567-2011, 2011.
Im, U., Markakis, K., Poupkou, A., Melas, D., Unal, A., Gerasopoulos, E., Daskalakis, N., Kindap, T., and Kanakidou, M.: The impact of temperature changes on summer time ozone and its precursors in the Eastern Mediterranean, Atmos. Chem. Phys., 11, 3847–3864, doi:10.5194/acp-11-3847-2011, 2011.
Im, U., Markakis,K., Koçak, M., Gerasopoulos, E., Daskalakis, N., Mihalopoulos, N., Poupkou, A., Kindap, T., Unal, A., and Kanakidou, M.: Summertime aerosol chemical composition in the Eastern Mediterranean and its sensitivity to temperature, Atmos. Environ., 50, 164–173, 2012.
IPCC, Contribution of Working Groups I, II and III to the Fourth Assessment Report of the Intergovernmental Panel on Climate Change Core Writing Team, edited by: Pachauri, R. K. and Reisinger, A., IPCC, Geneva, Switzerland, 104 pp., 2007.
Jacob, D. J. and Winner, D. A.: Effect of climate change on air quality, Atmos. Environ., 43, 51–63, 2009.
Jacob, D., Barring, L, Christensen, O. B., Christensen, J. H., de Castro, M., Deque, M., Giorgi, F., Hagemann, S., Hirschi, M., Jones, R., Kjellstrom, E., Lenderingk, G. Rockel, B., Sanchesz,

ACPD
12, 12245–12285, 2012

The impact of differences in large-scale circulation output

A. M. M. Manders et al.

E., Schar, C., Seneviratne, S. I., Somot, S., van Ulden, A., and Van den Hurk, B.: An intercomparison of regional climate models for Europe: model performance in present-day climate, Climatic Change, 81, 31–52, 2007.
Jimenez-Guerrero, P., Jose Gomez-Navarro, J., Jerez, S., Lorente-Plazas, R., Garcia-Valero, J. A., and Montavez, J. P.: Isolating the effects of climate change in the variation of secondary inorganic aerosols (SIA) in Europe for the 21st century (1991–2100), Atmos. Environ., 45, 1059–1063, 2011.
Kuenen., J., Denier van der Gon, H., Visschedijk, A., van der Brugh, H., and van Gijlswijk, R.: MACC European emisison inventory for the years 2003–2007, TNO report, UT-2011-00588, 2011.
Lenderink, G, Van den Hurk, B., Van Meijgaard, E., Van Ulden, A. P., and Cuijpers, J.: Simulation of present-day climate in RACMO2: first results and model developments, KNMI technical report TR 252, 2003.
Liao, K.-J., Tagaris, E., Manomaiphiboon, K., Wang, C., Woo, J.-H., Amar, P., He, S., and Russell, A. G.: Quantification of the impact of climate uncertainty on regional air quality, Atmos. Chem. Phys., 9, 865–878, doi:10.5194/acp-9-865-2009, 2009.
Manders, A. M. M., Schaap, M., and Hoogerbrugge, R.: Testing the capability of the chemistry transport model LOTOS-EUROS to forecast PM_{10} levels in the Netherlands, Atmos. Environ., 43, 4050–4059, 2009.
Manders, A. M. M., van Ulft, B., van Meijgaard, E., and Schaap, M.: Coupling of the air quality model LOTOS-EUROS to the climate model RACMO, Dutch National Research Programme Knowledge for Climate Technical Report KFC/038E/2011, ISBN 978-94-90070-00-7, 2011.
Mitchell, J. F. N., Johns, T. C., Eagles, M., Ingram, W. J., and Davis, R. A.: Towards the construction of climate change scenarios, Climatic Change, 41, 547–581, 1999.
Mues, A., Manders, A., Schaap, M., Kerschbaumer, A., Stern, R., and Builtjes, P.: Impact of the extreme meteorological conditions during the summer 2003 in Europe on particle matter concentrations – an observation and model study, Atmos. Environ., 55, 377–391, 2012.
Moriondo, M., Good, P., Durão, R., Bindi, M., Giannakopoulos, C., and Corte-Real, J.: Potential impact of climate change on fire risk in the Mediterranean area, Climate Research, 31, 85–95, doi:10.3354/cr031085, 2006.
Raes, F., Liao, H., Chen, W.-T., and Seinfeld, J. H.: Atmospheric chemistry-climate feedbacks, J. Geophys. Res. D, 115, 14 pp., doi:10.1029/2009JD013300, 2010.

ACPD
12, 12245–12285, 2012

Saarikoski, S., Sillanpaa, M, Sofiev, M., Timonen, H., Saarnio, K., Teinila, K., Kukkonen, J., and Hillamo, R.: Chemical composition of aerosols during a major biomass burning episode over northern Europe in spring 2006: Experimental and modeling assessments, Atmos. Environ., 41, 3577–3589, 2006.

Schaap, M., Timmermans, R. M. A., Sauter, F. J., Roemer, M., Velders, G. J. M., Boersen, G. A. C., Beck, J. P., and Builtjes, P. J. H.: The LOTOS-EUROS model: description, validation and latest developments, Int. J. Environ. Pollut., 32, 270–290, 2008.

Tagaris, E., Manomaiphiboon, K., Liao, K.-J. Leung, L. R., Woo, J. H., He, S., Amar, P., and Russell, A. G.: The impact of global climate change and emissions on regional ozone and fine particulate matter concentrations over the US, J. Geophys. Res.,-Atmos., 112, D14312, doi:10.1029/2006JD008262, 2007.

Tai, A. P. K., Mickely, L. R., and Jacob, D. J.: Correlations between fine particulate matter ($PM_{2.5}$) and meteorological variables in the United States: implications for the sensitivity of $PM_{2.5}$ to climate change, Atmos. Environ., 44, 3976–3984, doi:10.1016/j.atmosenv.2010.06.060, 2010.

Van Loon, M., Vautard., R., Schaap, M., Bergstrom, R., Bessagnet, B., Brandt, J., Builtjes, P. H. J., Christensen, H. J., Cuvelier, C., Graff, A., Jonson, J. E., Krol, M., Langner, J., Roberts, P., Rouil, L., Stern, R., Tarrason, L., Thunis, P., Vignati, E., White, L., and Wind, P.: Evaluation of long-term ozone simulations from seven regional air quality models and their ensemble, Atmos. Environ., 41, 2083–2097, 2007.

Van Meijgaard, E., Van Ulft, L. H., Van de Berg, W. J., Bosveld, F. C., Van den Hurk, B. J. J. M, Lenderink, G., and Siebesma, A. P.: The KNMI regional atmospheric climate model RACMO version 2.1. KNMI Technical report, TR-302, 2008.

van Ulden, A. P. and van Oldenborgh, G. J.: Large-scale atmospheric circulation biases and changes in global climate model simulations and their importance for climate change in Central Europe, Atmos. Chem. Phys., 6, 863–881, doi:10.5194/acp-6-863-2006, 2006.

Vautard, R., Beekmann, M., Desplat, J., Hodzic, A., and Morel, S.: Air quality in Europe during the summer of 2003 as a prototype of air quality in a warmer climate, C.R. Geoscience, 11–12, 747–763, 2007a.

Vautard, R., Builtjes, P. H. J., Thunis, P., Cuvelier, P., Bedogni, M., Bessagnet, B., Honore, C., Moussiopoulos, N., Pirovano, G., Schaap, M., Stern, R., Tarrason, L., and Wind, P.: Evaluation and intercomparison of Ozone and PM_{10} simulation by several chemistry transport models over four European Cities within the City Delta project, Atmos. Environ., 41, 173–188, 2007b.

Zhang, Y., Wen, X.-Y., and Jang, C. J.: Simulating chemistry-aerosol-cloud-radiation-climate feedbacks over the continental U.S. using the online-coupled Wather Research Forecasting Model with chemistry (WRF/Chem), Atmos. Environ., 44, 3568–3582, 2010.

ACPD

12, 12245–12285, 2012

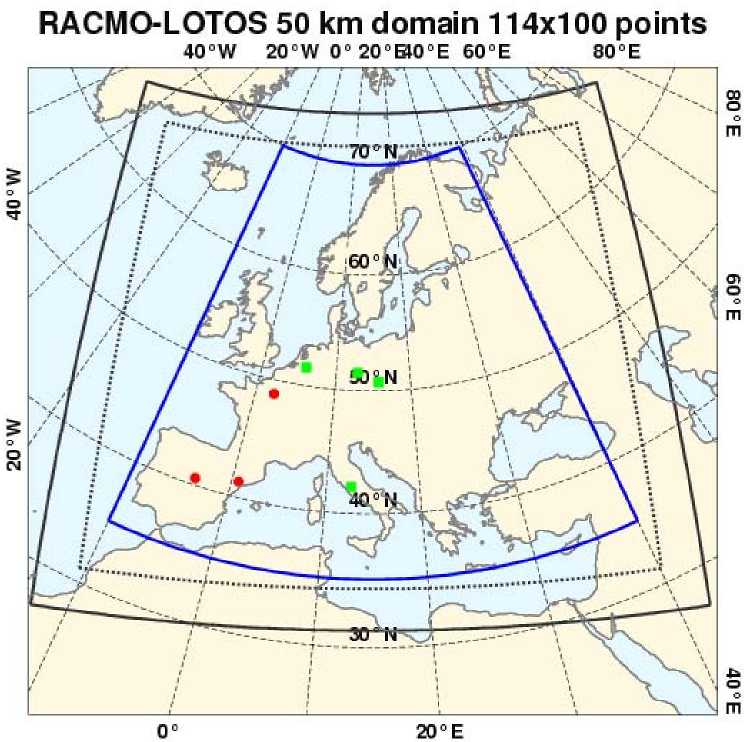

Fig. 1. RACMO domain in black, inner domain dashed, encompassing the LOTOS-EUROS domain (in blue). Points indicate locations that are used in the analysis below: red corresponds to cities, green to EMEP locations.

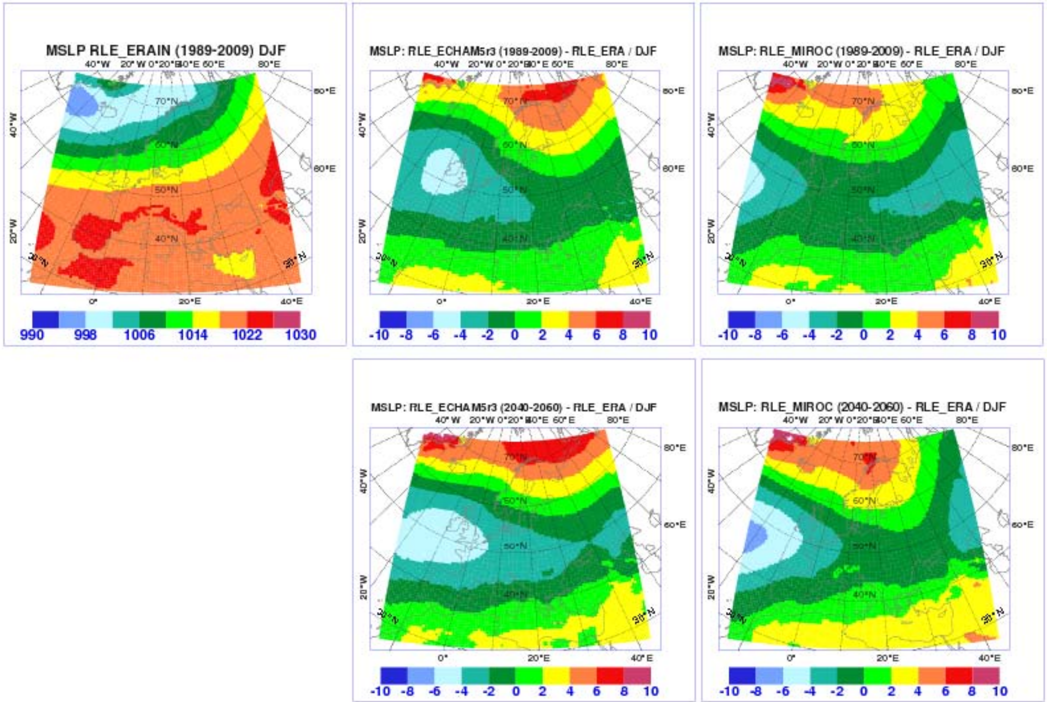

Fig. 2a. Average mean sea level pressure in RLE_ERA for Winter (December-January-February) in left-hand panel upper row. Central (right-hand) panels show differences in mslp between RLE_ECHAM5 (RLE_MIROC) and RLE_ERA for present-day (1989–2009) climate (top row) and future (2040–2060) climate (bottom row).

ACPD
12, 12245–12285, 2012

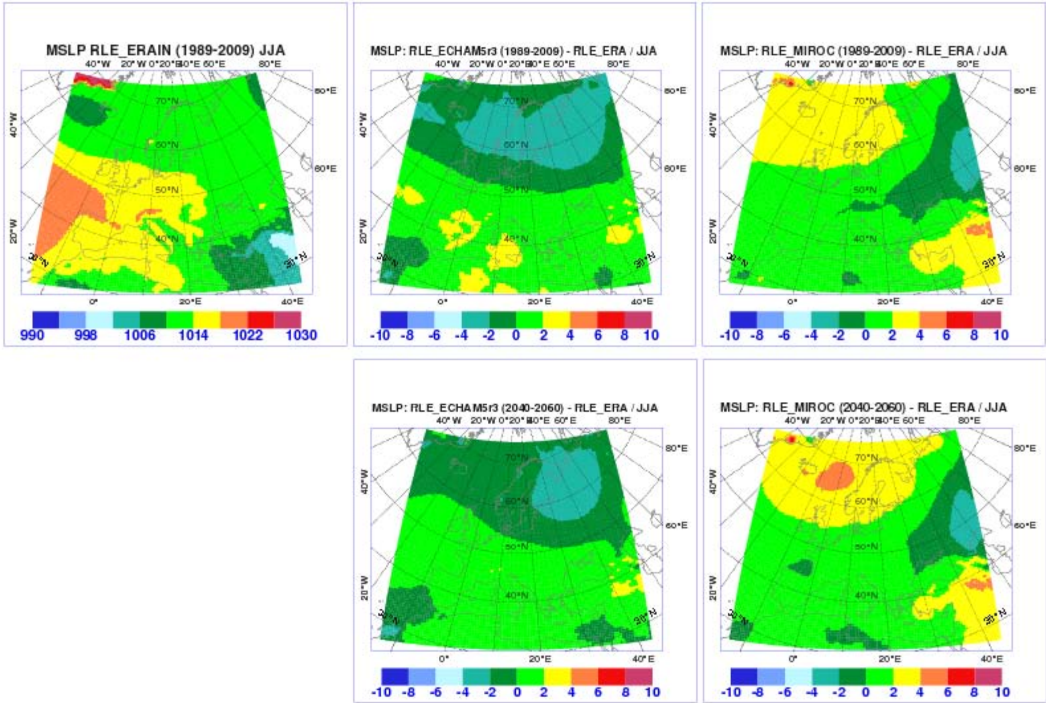

Fig. 2b. Like Fig. 2a but for Summer (June-July-August).

ACPD
12, 12245–12285, 2012

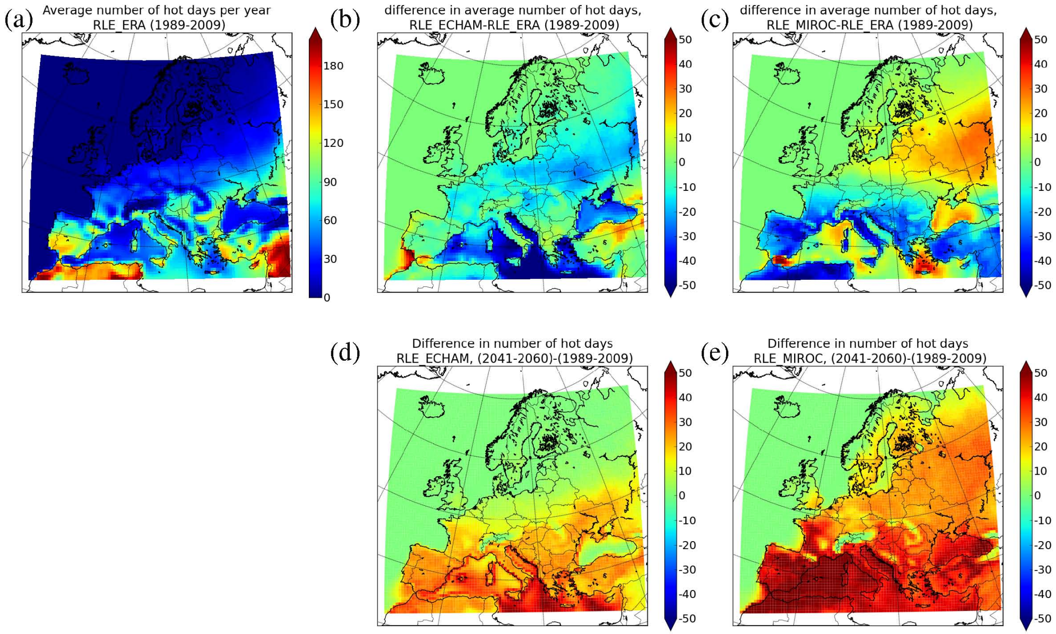

Fig. 3. Average number of summer days ($T_{max} > 25\,^{\circ}C$). Present day **(a)** RLE_ERA, **(b)** difference RLE_ECHAM-RLE_ERA, **(c)** difference RLE_MIROC-RLE_ERA and future minus present **(d)** RLE_ECHAM and **(e)** RLE_MIROC.

ACPD
12, 12245–12285, 2012

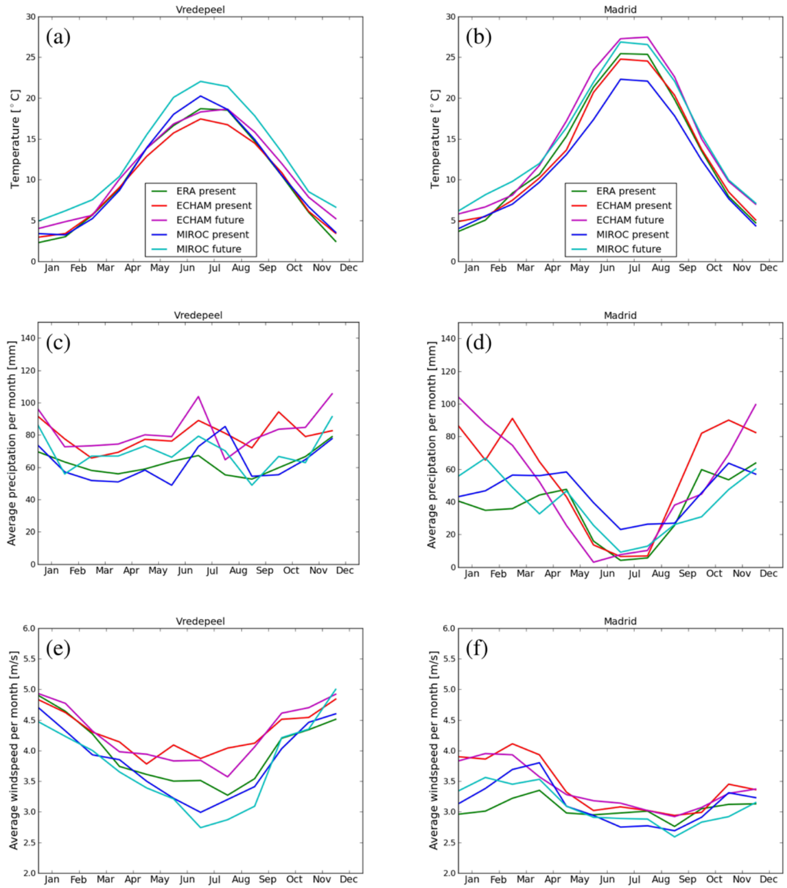

Fig. 4. Average annual cycles of monthly mean values for daily maximum temperature **(a, b)**, monthly mean precipitation **(c, d)** and monthly mean wind speed **(e, f)** at Vredepeel (left) and Madrid (right) derived from various downscaling runs experiments with RACMO2.

ACPD
12, 12245–12285, 2012

The impact of differences in large-scale circulation output

A. M. M. Manders et al.

Title Page
Abstract Introduction
Conclusions References
Tables Figures
◀◀ ▶▶
◀ ▶
Back Close
Full Screen / Esc
Printer-friendly Version
Interactive Discussion

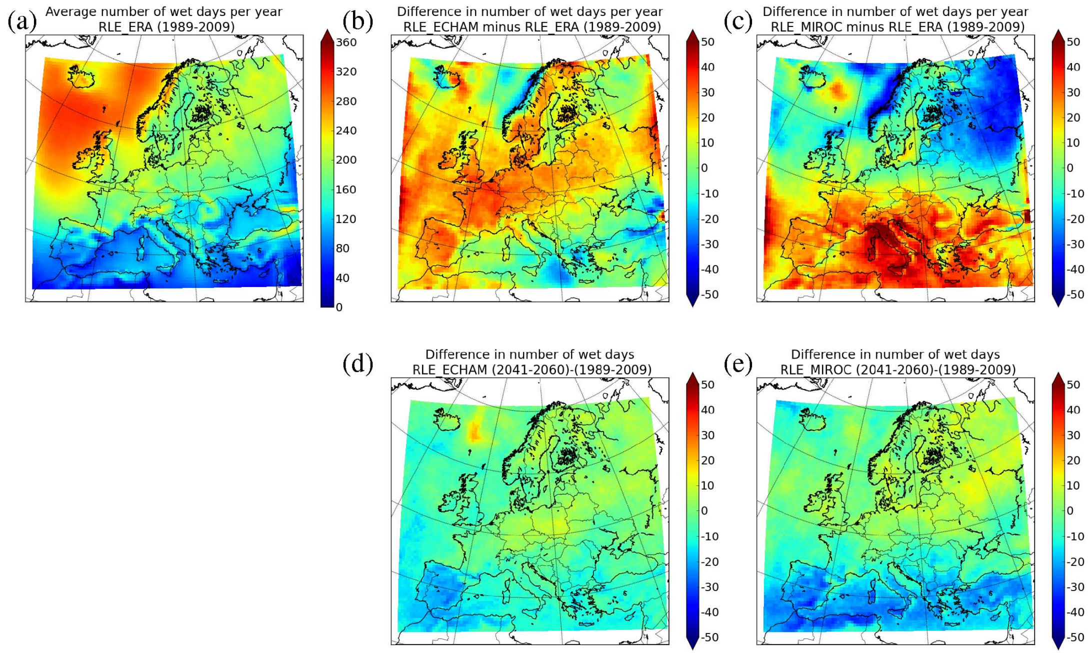

Fig. 5. Average number of wet for days. Present day-climate (**a**, RLE_ERA), differences between the simulations (**b**, RLE_ECHAM, **c**, RLE_MIROC)) and differences future minus present (**d**, RLE_ECHAM), (**e**, RLE_MIROC).

ACPD
12, 12245–12285, 2012

The impact of differences in large-scale circulation output

A. M. M. Manders et al.

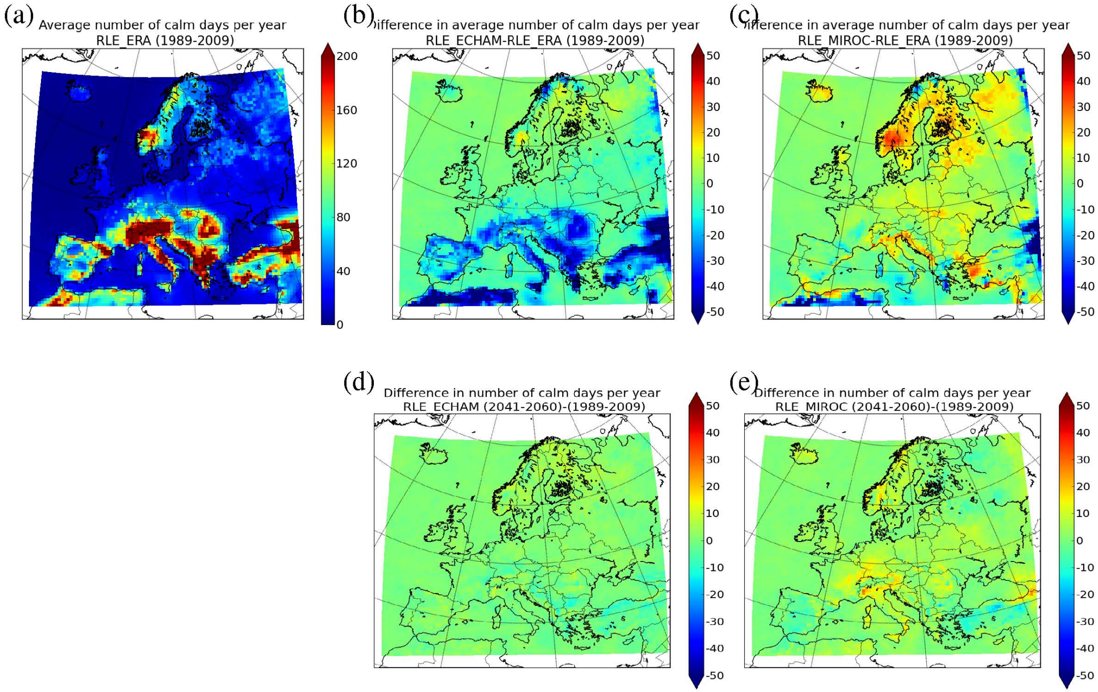

Fig. 6. Average number of calm days, **(a)** present-day RLE_ERA, **(b)** difference RLE_ECHAM-RLE_ERA, **(c)** difference RLE_MIROC-RLE_ERA, and future minus present **(d)** RLE_ECHAM, **(e)** RLE_MIROC.

ACPD
12, 12245–12285, 2012

The impact of differences in large-scale circulation output

A. M. M. Manders et al.

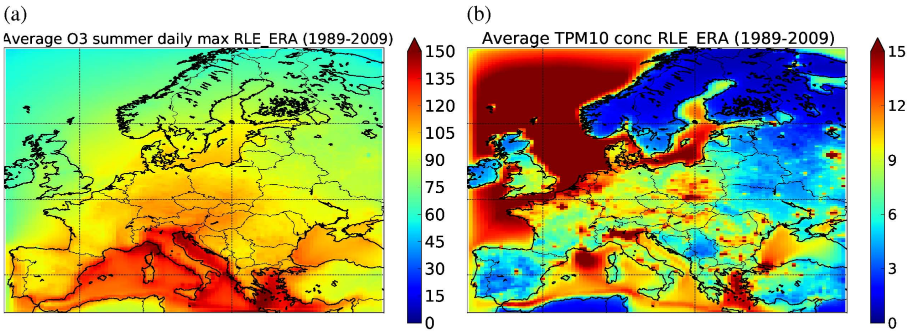

Fig. 7. Average O_3 summer maximum **(a)** and annual average total PM_{10} concentration **(b)** obtained with RLE_ERA (1989–2009).

ACPD
12, 12245–12285, 2012

The impact of differences in large-scale circulation output

A. M. M. Manders et al.

Title Page
Abstract | Introduction
Conclusions | References
Tables | Figures
◀| |▶
◀ ▶
Back | Close
Full Screen / Esc
Printer-friendly Version
Interactive Discussion

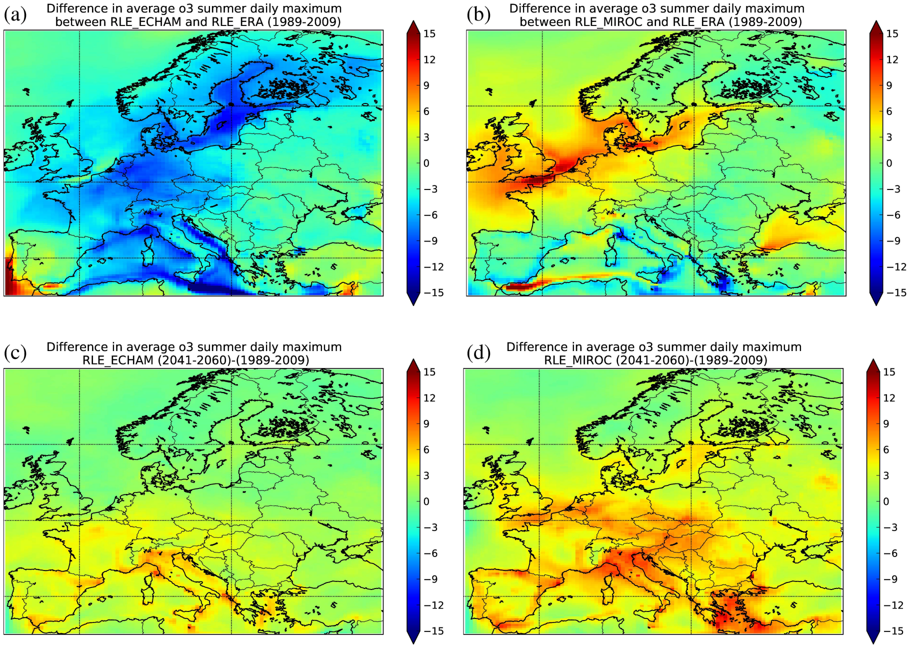

Fig. 8. Difference between average O_3 summer maximum concentrations. Upper panels: differences present-day with RLE-ERA run, lower panels difference between future and present day. Left: RLE_ECHAM, right: RLE_MIROC.

ACPD
12, 12245–12285, 2012

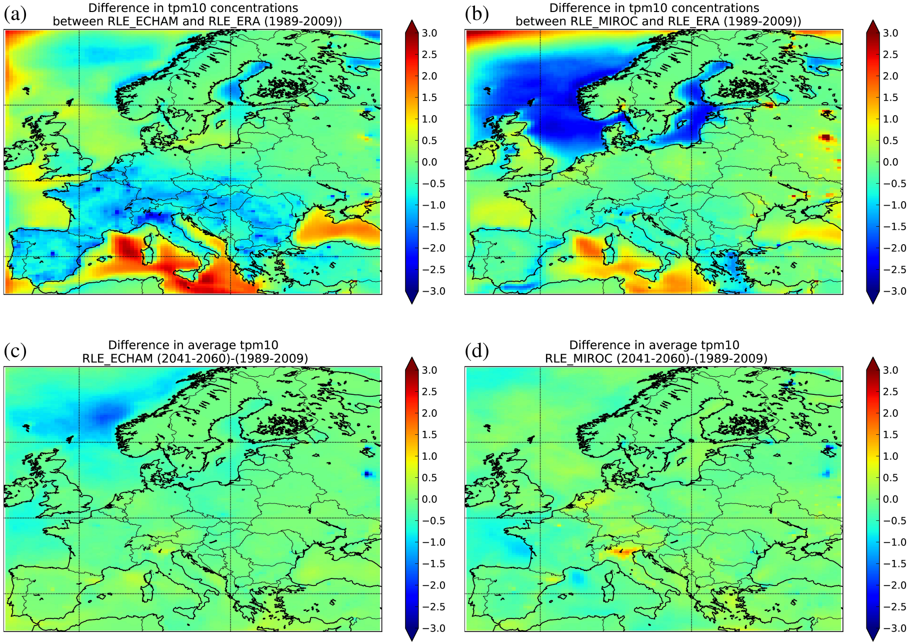

Fig. 9. Difference total PM_{10} concentrations. Upper panels: differences present-day with RLE-ERA, lower panels difference between future and present day. Left: RLE_ECHAM, right: RLE_MIROC.

ACPD
12, 12245–12285, 2012

The impact of differences in large-scale circulation output

A. M. M. Manders et al.

ACPD
12, 12245–12285, 2012

The impact of differences in large-scale circulation output

A. M. M. Manders et al.

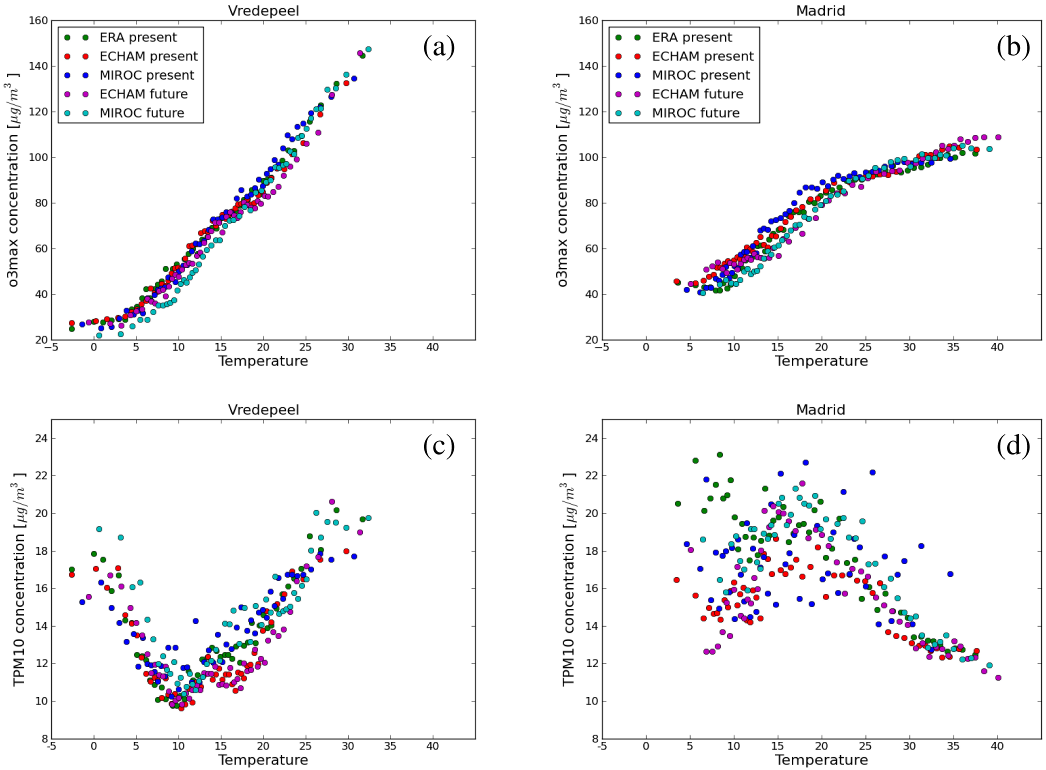

Fig. 10. Average relationship between ozone daily maximum or total PM_{10} from LOTOS-EUROS and daily maximum temperature for the meteorologies downscaled with RACMO.

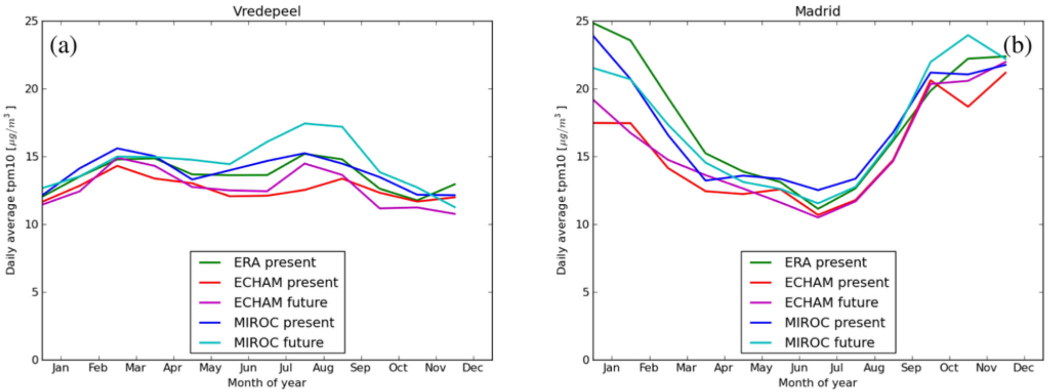

Fig. 11. Simulated daily mean PM_{10} concentrations for Vredepeel **(a)** and Madrid **(b)** averaged over 20 yr.

ACPD
12, 12245–12285, 2012

The impact of differences in large-scale circulation output

A. M. M. Manders et al.